Molecular Characterization, Expression and Functional Analysis of Yak IFITM3 Gene

Haipeng Wang
Southwest Minzu University
Li Wang (qinxin916@aliyun.com)
Southwest Minzu University https://orcid.org/0000-0001-8267-9309
Juan Li
Southwest Minzu University
Fang Fu
Southwest Minzu University
Yao Zheng
Southwest Minzu University
Ling Zhang
Southwest Minzu University

Research

Keywords: IFITM3, Yak, Hepatocyte, HepG2, PI3K/Akt, Ferroptosis

Posted Date: April 27th, 2021

DOI: https://doi.org/10.21203/rs.3.rs-447052/v1

Molecular characterization, expression and functional analysis of yak *IFITM3* gene

Haipeng Wang[1,2], Li Wang[1,2*], Juan Li[1,2], Fang Fu[1,2], Yao Zheng[1,2], Ling Zhang[1,2]

Abstract

Background

IFITM3 is interferon-induced transmembrane 3, which plays an extremely key role in anti-proliferation, anti-virus and anti-tumor diseases. To expand our understanding of the role of IFITM3 in yak, this experiment studied its function.

Results

Firstly, the yak (*Bos grunniens*) *IFITM3* (*BgIFITM3*) gene contained a 5'-untranslated region (UTR) (25 bp), a coding region (441 bp), and a 3'-UTR (115 bp). The expression of *BgIFITM3* gene in liver was significantly higher than that in heart, spleen, lung and kidney (P <0.01). BgIFITM3 protein was localized on the yak hepatocyte membrane, and its expression level was increased first and then stabilized from 1 day to 5 years of age. Moreover, the prokaryotic expression vector of BgIFITM3 protein was constructed and expressed successfully, with a molecular weight of 19.5 kDa. Besides, the activity of yak hepatocyte was significantly inhibited after treating with BgIFITM3 protein (10 and 20 μg/mL) (P <0.01). The expression levels of *ERBB-2, IRS-1, PI3KR-1, AKT-1* and *MAPK-3* were significantly lower after treating with 20 μg/mL BgIFITM3 protein (P <0.05). Finally, the activity of HepG2 cells was significantly inhibited after treating with BgIFITM3 protein (1, 10 and 20 μg/mL) (P <0.05). While the cloning ability and migration ability of HepG2 cells were significantly inhibited after treating with 10 μg/mL BgIFITM3 protein (P <0.05). The mitochondria of HepG2 cells were concentrated, cristae widened, and the double film density of mitochondria was increased after treating with 10 μg/mL BgIFITM3 protein. After 10 μg/mL BgIFITM3 protein treating, the expression levels of *VDAC-2, VDAC-3*, *p53* genes were significantly increased, but the expression level of *GPX-4* gene was significantly decreased (P <0.01).

Conclusion

Taken together, the BgIFITM3 protein could inhibit the proliferations of yak hepatocyte and HepG2 cells by regulating the PI3K/Akt pathway or ferroptosis-related genes, respectively. These results benefit for further study of the function of BgIFITM3 protein.

Keywords

IFITM3, Yak, Hepatocyte, HepG2, PI3K/Akt, Ferroptosis

Background

IFITM3 is interferon-induced transmembrane protein 3, also known as fragilis or I-8U is a 15-kDa protein encoded on human chromosome 11 and mouse chromosome 7 and is induced by type I, II and III IFNs **[1-3]**. IFITM3 is mainly located on endolysosomal membrane, and placed an inhibitory role at an early stage of viral replication **[4]**. It can inhibit the entry of viruses by preventing virus fusion with endolysosomal membrane **[5-8]**. Among all IFITM family proteins, IFITM3 has the highest antiviral activity and is one of the most popular proteins in human antiviral research **[9-12]**. IFITM3 can resist viral infection in various ways, including: changing the characteristics of cell membrane and interacting with multiple viral receptors on cell membrane **[13, 14]**. Overexpression of human IFITM3 restricts the infection, replication and proliferation of vaccinia virus, mainly by interfering with the entry of virus in a low pH-dependent manner **[15]**. Recently, IFITM3 can regulate γ-secretase in human Alzheimer's disease **[16]**. Swine IFITM3 had an inhibitory effect for PRRS virus, Japanese B type encephalitis virus and FMDV **[17-19]**. Avian IFITM3 had a significant inhibitory effect on avian influenza virus **[18-19]**.

Recently, an increasing number of studies have focused on the role of IFITM3 in tumorigenesis and development. IFITM3 was significantly overexpressed in many tumors including colon cancer, astrocytoma, human glioma, myeloid leukemia and prostate cancer, as well as liver cancer **[20-23]**. The yak (*Bos grunniens*) is widespread in the largest and harshest highland in the world, the Qinghai–Tibet Plateau. Yak living at high altitudes. The high-altitude area has the characteristics of low oxygen, low temperature, strong radiation, etc. And these characteristics can cause changes in the body's immune function **[24-26]**. Indeed, the yak has become strongly integrated into Tibetan socio-cultural life and plays a significant economic role in the mountainous regions. At present it has become a symbol of plateau animal husbandry **[27-29]**. In this study, The *BgIFITM3* gene was cloned and identified, and the purified yak IFITM3 protein was obtained by prokaryotic expression, to study the function of BgIFITM3 protein.

Materials & Methods

Animal and Cell culture

The heart, liver, spleen, lung, and kidney were collected from Maiwa yak (1 day, 15 months

and 5 years old) in Sichuan Province, China. Yak was slaughtered under anesthesia and every effort was made to minimize the risk of illness. The excised tissue was frozen in liquid nitrogen for transport and finally stored at -80 ℃. Another part of the yak liver tissue was placed in saline containing penicillin-streptomycin and returned to the laboratory at 4 ℃, and the yak hepatocyte were separated by collagenase digestion. HepG2 cells were donated by Chengdu Medical College. Yak hepatocyte were cultured in DMEM/F12 medium at 37 ℃. HepG2 cells were cultured in DMEM medium at 37 ℃. The cells were digested by 0.25% trypsin (Sangon Biotech, China).

Gene cloning

Total RNA was extracted from each tissue and cells. The concentration and OD value were measured by an UV-visible spectrophotometer. cDNA samples were synthesized according to the instructions of the PrimeScript™ RT reagent Kit (TaKaRa, Japan). The quality of cDNA was detected by *Y-β-actin* gene (Table 1). The cDNA was stored at -20 ℃. The primers of *BgIFITM3* gene (F: GAAAAGGAAACTTAGGAGAAATC; R: ACTGCCTCGGGCTGTG) were designed in NCBI. PCR conditions were as follows: 98 ℃ for 2 min, then 98 ℃ for 10 s, 54 ℃ for 10 s, 72 ℃ for 10 s, 35 cycles, followed by 72 ℃ for 2 min, 4 ℃ forever.

Table 1 Fluorescence quantitative PCR primer sequence and reaction conditions

Primer name	Primer sequence（5'→3'）	Tm/℃
Y-IFITM3	F：TCAAGGAGGAGCACGAGG R：TAGGCGAATGCCACGAA	65.0
Y-ERBB-2	F：CTCTGGTCACCTACAACA R：TCCGTAGACAGATAGTTG	53.4
Y-IRS-1	F：TGGACAAACGGGGTAGGG R：TAATAGCAGTCGGAGGGG	53.4
Y-PI3KR-1	F：AAACCACCAAAACCCACT R：GCTCTGCTGAAAAACTCG	53.4
Y-AKT-1	F：CCCGCCCTTCAAGCCTCA R：TCGCTGTCCACCCCCTCC	53.4
Y-RAF-1	F：CACTGTTGGTGATGGCGG R：CAGAGGAGGGGCTGGAGG	53.4
Y-MAPK-3	F：ATCAACACCACCTGCGAC R：GGGCAAGACCGAAATCAC	53.4
H-MMP2	F：TGGCAAGGAGTACAACAGC R：GGAAGCGGAATGGAAAC	53.5

H-MMP9	F：CGACGTCTTCCAGTACCGAG R：TTGTATCCGGCAAACTGGCT	57.3
H-FTH-1	F：GAACTACCACCAGGACTC R：TTCTTCAAAGCCACATC	54.0
H-VDAC-2	F：AAGTGGTGTGAGTATGGT R：CTTTTCTTTCCTGTGTTT	54.0
H-VDAC-3	F：GACTTACCTTCACCCAGA R：ACACTAAAACAATCCCGT	54.0
H-GPX-4	F：TGTGGAAGTGGATGAAGA R：TAGAAATAGTGGGGCAGG	54.0
H-P53	F：GTTGATTCCACACCCCCG R：TCCAAATACTCCACACGC	54.0
Y-β-actin	F：CTTCGAGCAGGAGATGGC R：CCGTGTTGGCGTAGAGGT	53.4
Y-GAPDH	F：ATCTGACCTGCCGCCTGGAG R：GACGCCTGCTTCACCACCTTC	54.0
H-GAPDH	F：TGTTGCCATCAATGACCCCTT R：CTCCACGACGTACTCAGCG	51.0

Y represents yak-related genes; H represents human related genes

F. Sense primer; R. Antisense primer

Bioinformatics analysis

PCR products were sequenced, and the sequence of *BgIFITM3* gene was analyzed by BLAST program. Amino acid sequence was predicted by ORF Finder program. The homology was analyzed by DNAMAN software. The evolutionary tree was constructed by MEGA6 software. The nucleotide sequences of *IFITM3* from various species were compared by pairwise alignment using the Species Demarcation Tool. The basic physical and chemical properties were analyzed by ProtParam. Protein domains, signal peptides, transmembrane structure, secondary structure and tertiary structure were predicted by Conserved Domains, SignalP 5.0 Server, SOPMA, SWISS-MODEL, respectively.

Construction of prokaryotic expression vector

The *BgIFITM3* gene amplification product was recovered by DNA Gel Extraction Kit (OMEGA, United States), and cloned to pMD19-T vector (Takara, Japan). The positive clone colonies were screened for identification. The correct colony was submitted for sequenced. The correct plasmid and pET-28a (Solarbio, China) were digested with *Hin*d-III (TaKaRa, Japan) and

*Eco*R-I (TaKaRa, Japan). T_4 DNA ligase (TaKaRa, Japan) was added to ligate overnight at 16 ℃. The ligation product was named pET28a-BgIFITM3.

Expression and purification of recombinant plasmid

The pET28a-BgIFITM3 was transformed into BL21(DE3) competent cells (Sangon Biotech, China) and cultured overnight in LB agar medium. Monoclonal white plaques were picked for expanding culture. 1.4 mM/L IPTG was added to culture 12 h. The fusion expression product was identified by SDS-PAGE. BgIFITM3 protein was purified by nickel column method, and the concentration of purified protein was detected by BCA Protein Assay Kit (TIANGEN, China).

Western Blot

The total liver protein of yak was extracted by Tissue or Cell Total Protein Extraction Kit (Sangon Biotech, China). The mouse anti-His tag MAb (1:4000, CWBIO, China) was used as the primary antibody, and the HRP-conjugated goat anti-mouse IgG (1:10000, CWBIO, China) was used as the secondary antibody to identified purified BgIFITM3 protein. The Rabbit Anti-Fragilis (1:1500, Bioss, China) was used as the primary antibody, and the HRP-conjugated Goat Anti-Rabbit IgG (1:10000, Sangon Biotech, China) was used as the secondary antibody to detected the expression of IFITM3 protein in yak liver tissues of different age. The target protein was separated by 15% SDS-PAGE electrophoresis and transferred to the PVDF membrane (Sangon Biotech, China), and blocked with 5% milk at room temperature for 1 h. The primary antibody was incubated at 4 ℃ for 12 h, and the secondary antibody was incubated at room temperature for 1.5 h. Finally, the PVDF membrane was rinsed with a ECL luminescent reagents (Sangon Biotech, China) for 5 min in dark.

Immunohistochemistry

The yak livers of different growth stages were taken out of 4% paraformaldehyde fixative solution and made into paraffin sections. Rabbit Anti-Fragilis (1:100, Bioss, China) was used as the primary antibody, and polymerized goat anti-rabbit IgG (1:200, ZSGB-BIO, China) was used as the secondary antibody. The relative average optical density value of IFITM3 expression was determined by Image-Pro Plus 6.0.

CCK-8 assay

2×10^3 Cells were plated onto a 96-well culture plate and incubated overnight. Yak hepatocyte were treated with different concentrations of BgIFITM3 protein (0, 10 and 20 μg/mL). While,

HepG2 cells were treated with different concentrations of BgIFITM3 protein (0, 1, 10 and 20 μg/mL). Three replicate wells were set for each concentration. The cell viability was detected according to the instruction of CCK-8 kit (Sangon Biotech, China).

Colony formation assay

HepG2 Cells were plated onto a 6-well culture plate. Then, HepG2 cells were treated by BgIFITM3 protein (0, 1 and 10 μg/mL), and incubated in 37 ℃, 5% CO_2 incubator. HepG2 cells were fixed with 4% paraformaldehyde (biosharp, China) for 20 min and stained with crystal violet for 15 min. HepG2 cells were rinsed with double distilled water and taken pictures count.

Scarification test

HepG2 Cells were plated onto a 24-well culture plate. When the cell fusion reached 70%, each well was scratched and observed by using 10 μL pipette tip. After 24 h of treatment with BgIFITM3 protein (0, 1 and 10 μg/mL) in the serum-free medium, the scratches of each well were photographed and the cells were measured scratch width after migration.

Transmission electron microscope observation

HepG2 Cells were plated onto a 6-well culture plate and incubated overnight. 10 μg/mL BgIFITM3 protein were added to each well. The HepG2 cells were collected by trypsinization. Then the HepG2 cells were fixed, dehydrated, infiltrated, embedded, sectioned, stained, and observed by the JEM-1400PLUS transmission electron microscope.

Quantitative Real-time PCR (qRT-PCR)

BgIFITM3 genes in 5 tissues (heart, liver, spleen, lung and kidney) of three ages yak (1 day, 15 months and 5 years old) were detected by qRT-PCR. The expression level of *IFITM3* gene in various tissues of yak was measured by $2^{-\Delta\Delta Ct}$ method. Yak hepatocyte were treated by BgIFITM3 protein (0, 10 and 20 μg/mL), and HepG2 cells were treated by BgIFITM3 protein (0, 1 and 10 μg/mL). The cells were digested and collected after BgIFITM3 protein treating. The transcription level of each genes was detected by qRT-PCR. With *GAPDH* as the internal reference, and transcription levels were calculated by $2^{-\Delta\Delta Ct}$ method. The reaction system was 10 μL: 5.2 μL TB Green® Premix Ex Taq^{TM} II (TaKaRa, Japan), 0.8 μL of the upstream and downstream primers (10 mmol·L^{-1}), 1 μL sample, and ddH_2O 2.2 μL. qRT-PCR conditions were as follows: 95 ℃ for 2 min, then 95 ℃ for 15 s, annealing for 20 s, 39 cycles, followed by 65 ℃ for 5 s. The primers were shown in Table 1.

Statistical analysis

All data were analyzed by SPSS 26.0 and presented as mean ± SD of three independent experiments. GraphPad Prism 8.0 was used to plot gene expression profiles. One asterisk and two asterisks indicated P <0.05 and P <0.01 between groups, respectively.

Results

Cloning and Bioinformatics Analysis of *BgIFITM3* Gene

A 581 bp clear target band was obtained and sequenced by PCR amplification (Fig. 1a). The complete coding sequence (CDS) of *BgIFITM3* was 441 bp in length, encoding for a putative protein of 146 amino acids. The *BgIFITM3* gene had the 98.9% homology with common cattle, and had the 53.7% homology with frogs. Phylogenetic tree analysis results showed that the *BgIFITM3* gene was the closest to the evolutionary distance of the ordinary cattle, and the furthest from the amphibians (Fig. 1b-c). Collectively, these results suggested that IFITM3 was highly conserved in the same genus.

The BgIFITM3 protein had a molecular weight of 36.957 kDa, a theoretical isoelectric point pI of 5.15. The instability index of BgIFITM3 protein was 60.23, and the total average hydrophilicity was 0.928. The BgIFITM3 protein was a hydrophilic protein and transmembrane protein, but it had not a signal peptide. The BgIFITM3 protein had 25 Thr sites and a highly conserved structural functional domain CD225.

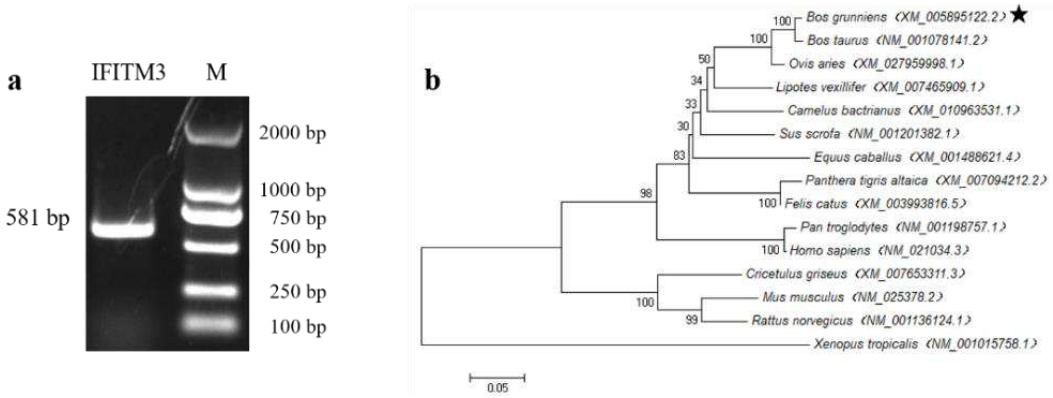

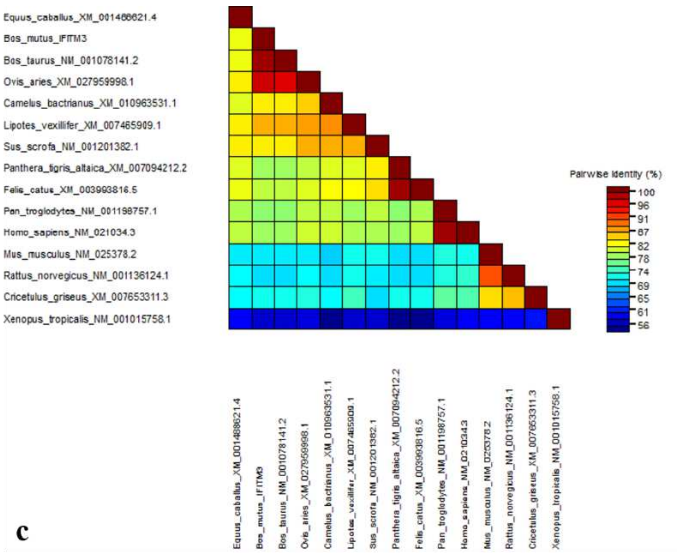

Fig. 1 Analysis of *BgIFITM3* Gene. **a** Result for PCR amplification of *BgIFITM3*. Note: M. DL2000 DNA Marker; IFITM3. *BgIFITM3* gene. **b** Phylogenetic tree based on *IFITM3* gene. **c** The nucleotide sequences of *IFITM3* from various species were compared by pairwise alignment

Transcription levels of BgIFITM3 gene in yak tissues

The transcription level of *BgIFITM3* gene in the liver had the highest in 15 months old, followed by higher in 5 years old, and lower in 1 day old, and the difference was extremely significant between 1 day and 15 months, 1 day and 5 years old (P <0.01). The transcription level of *BgIFITM3* gene in the spleen had the highest in 1 day old, followed by higher in 5 years old, and lower in 15 months old, and the difference was extremely significant between 1 day and 15 months, 1 day and 5 years old (P <0.01). The transcription level of *BgIFITM3* gene in the lung had the highest in 15 months old, followed by higher in 1 day old, and lower in 5 years old, and the difference was significantly between 1 day and 5 years old, 15 months and 5 years old (P <0.05). The transcription level of *BgIFITM3* gene in the kidney had the highest in 1 day old, followed by higher in 15 months old, and lower in 5 years old, and the difference was significantly between 1 day and 5 years old (P <0.05). There was no obvious difference of the transcription level of *BgIFITM3* gene in the heart between different ages. (Fig. 2a-e).

The transcription level of *BgIFITM3* gene in the liver was all extremely significantly higher than the heart, spleen, lung and kidney (P <0.01). While, the transcription level of *BgIFITM3* gene was higher in the heart, and lower in the yak spleen, lung and kidney (Fig. 2f-h). Collectively, these results suggested that the transcription level of *BgIFITM3* gene had tissue differences.

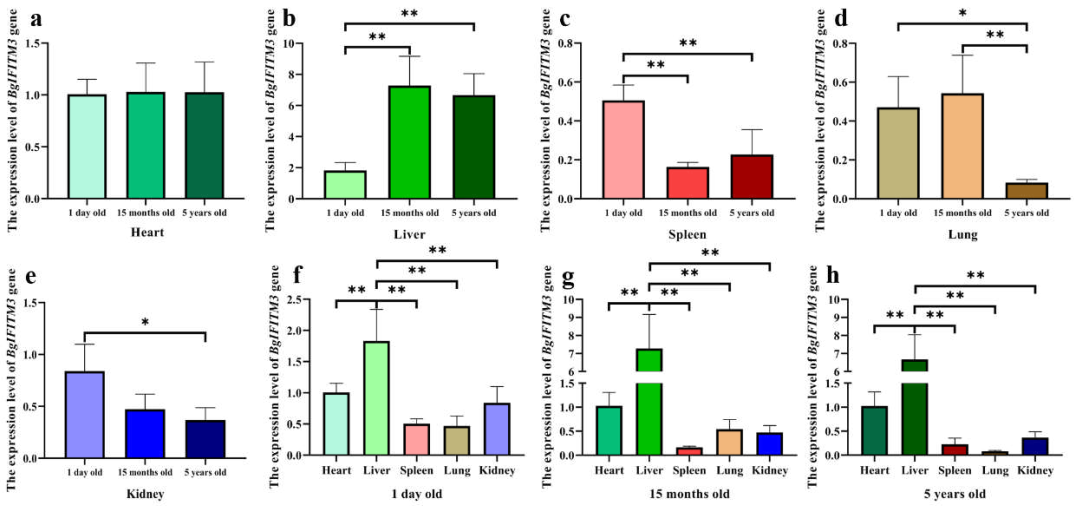

Fig. 2 The expression levels of *BgIFITM3* in different tissues of the yak. **a** The expression level of *BgIFITM3* gene in heart. **b** The expression level of *BgIFITM3* gene in liver. **c** The expression level of *BgIFITM3* gene in spleen. **d** The expression level of *BgIFITM3* gene in lung. **e** The expression level of *BgIFITM3* gene in kidney. **f** The expression level of *BgIFITM3* gene in 1 day old. **g** The expression level of *BgIFITM3* gene in 15 months old. **h** The expression level of *BgIFITM3* gene in 5 years old. Values are expressed as mean ± SD of n = 3. * P <0.05, ** P <0.01

Prokaryotic expression and identification of BgIFITM3 protein

The recombinant strain pET28a-BgIFITM3/DE3 was induced by IPTG and detected by SDS-PAGE. The results showed that the target recombinant protein band with a size of about 19.5 kDa appeared (Fig. 3a). After purification, SDS-PAGE showed a single band at about 19.5 kDa (Fig. 3b). Western blot identification results showed that specific bands appeared (Fig. 3c). Recombinant BgIFITM3 protein had been expressed and proven.

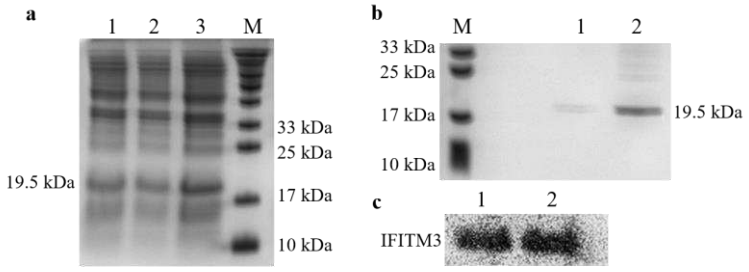

Fig. 3 Prokaryotic expression and identification of recombinant protein IFITM3. **a** Graph of BgIFITM3 protein induction. Note: M: The low molecular weight standard markers; 1-3: The precipitation pET28a-BgIFITM3/DE3 induced for 12 h. **b** Graph of BgIFITM3 protein purification. Note: M: The low molecular weight standard markers; 1-2: The purified recombinant protein pET28a-BgIFITM3. **c** Graph of BgIFITM3 protein identification. Note: M:

The low molecular weight standard markers; 1-2: The recombinant protein BgIFITM3

Localization and expression of BgIFITM3 protein in liver

BgIFITM3 protein was expressed in the yak livers at different growth stages, and the protein was mainly located on the yak hepatocyte membrane (Fig. 4a-f). Yellow or brownish yellow staining was judged as positive cells. With the increase of age, the relative average optical density value of IFITM3 expression showed the difference was significantly between 1 day and 15 months of age (P <0.05) (Fig. 4g-h). These results were consistent with the transcription level results.

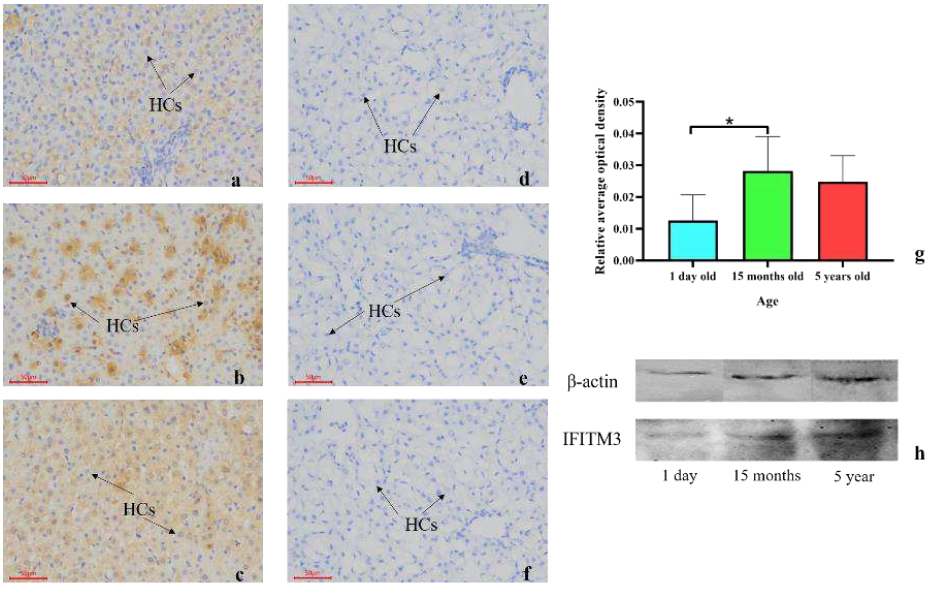

Fig. 4 Detection of IFITM3 expression distribution in yak liver tissues at different growth stages. **a-f** Cell localization of BgIFITM3 protein. **a** 1-day-old yak liver (200×). **b** 15-month-old yak liver (200×). **c** 5-year-old yak liver (200×). **d** Group a negative control. **e** Group b negative control. **f** Group c negative control. **g** Relative average optical density. **h** The expression level of IFITM3 protein in yak at different ages. HCs: Hepatocyte. Values are expressed as mean ± SD of n = 3. * P <0.05

The proliferation and PI3K/Akt related genes of yak hepatocyte

Purified BgIFITM3 protein was added to culture yak hepatocyte for 24 h, CCK-8 experiment results showed that after adding different concentrations of BgIFITM3 protein, the activity of yak hepatocyte gradually decreased with the increase in concentration. And the yak hepatocyte activity was significantly lower after treating with 20 μg/mL BgIFITM3 protein (P <0.01) (Fig. 5a). The results showed that addition of BgIFITM3 protein had an inhibitory effect on the proliferation of yak hepatocyte.

The expression levels of PI3K/Akt pathway related genes (*ERBB-2, IRS-1, PI3KR-1, AKT-1,*

RAF-1 and *MAPK-3*) in yak hepatocyte were detected by qRT-PCR. These results showed that the expression levels of *ERBB-2, IRS-1, PI3KR-1, AKT-1* and *MAPK-3* were significantly lower after treating with 20 μg/mL BgIFITM3 protein (P <0.05) (Fig. 5b-g). These results were consistent with the CCK-8 result.

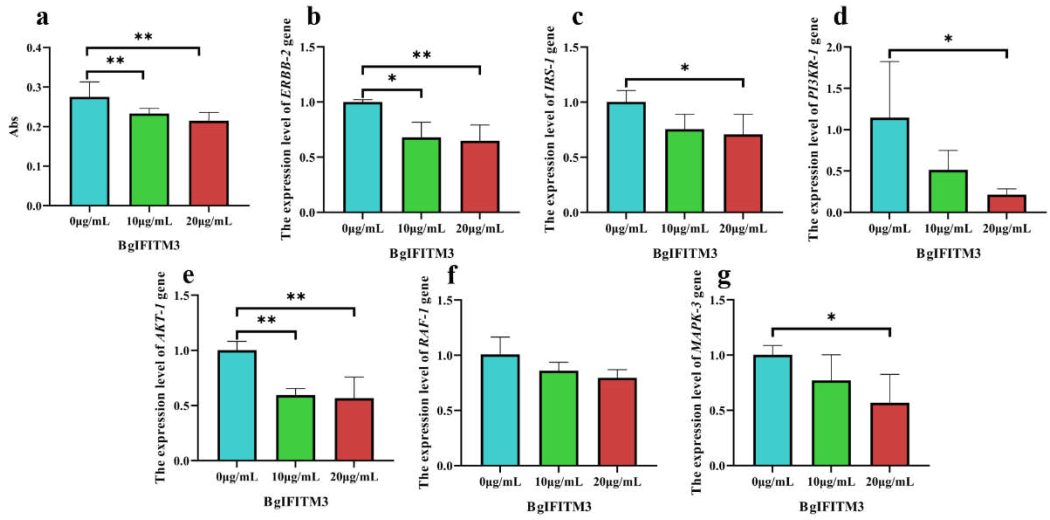

Fig. 5 Effects of different concentrations of BgIFITM3 protein on yak hepatocyte **a** The yak hepatocyte activity. **b** Expression of *ERBB-2*. **c** Expression of *IRS-1*. **d** Expression of *PI3KR-1*. **e** Expression of *AKT-1*. **f** Expression of *RAF-1*. **g** Expression of *MAPK-3*. Values are expressed as mean ± SD of n = 3. * P <0.05, ** P <0.01

The proliferation and migration of HepG2 cells

Purified BgIFITM3 protein was added to the cultured HepG2 cells for 24 h. The HepG2 cells activity was significantly lower after treating with 1 μg/mL BgIFITM3 protein (P <0.05), and it was extremely significantly lower after treating with BgIFITM3 protein (10 and 20 μg/mL) (P <0.01) (Fig. 6a). The results of the cell scratch experiment showed that the width of the cells was significantly higher after treating with 10 μg/mL BgIFITM3 protein (P <0.05) (Fig. 6b and e). The experimental results of HepG2 cells clone formation showed that the number of cell clones was 226.67, 149.33 and 55.00 after treating with BgIFITM3 protein (0, 1 and 10 μg/mL). The numbers of cell clones were extremely significant lower after treating with BgIFITM3 protein (1 and 10 μg/mL) (P < 0.01) (Fig. 6c and d).

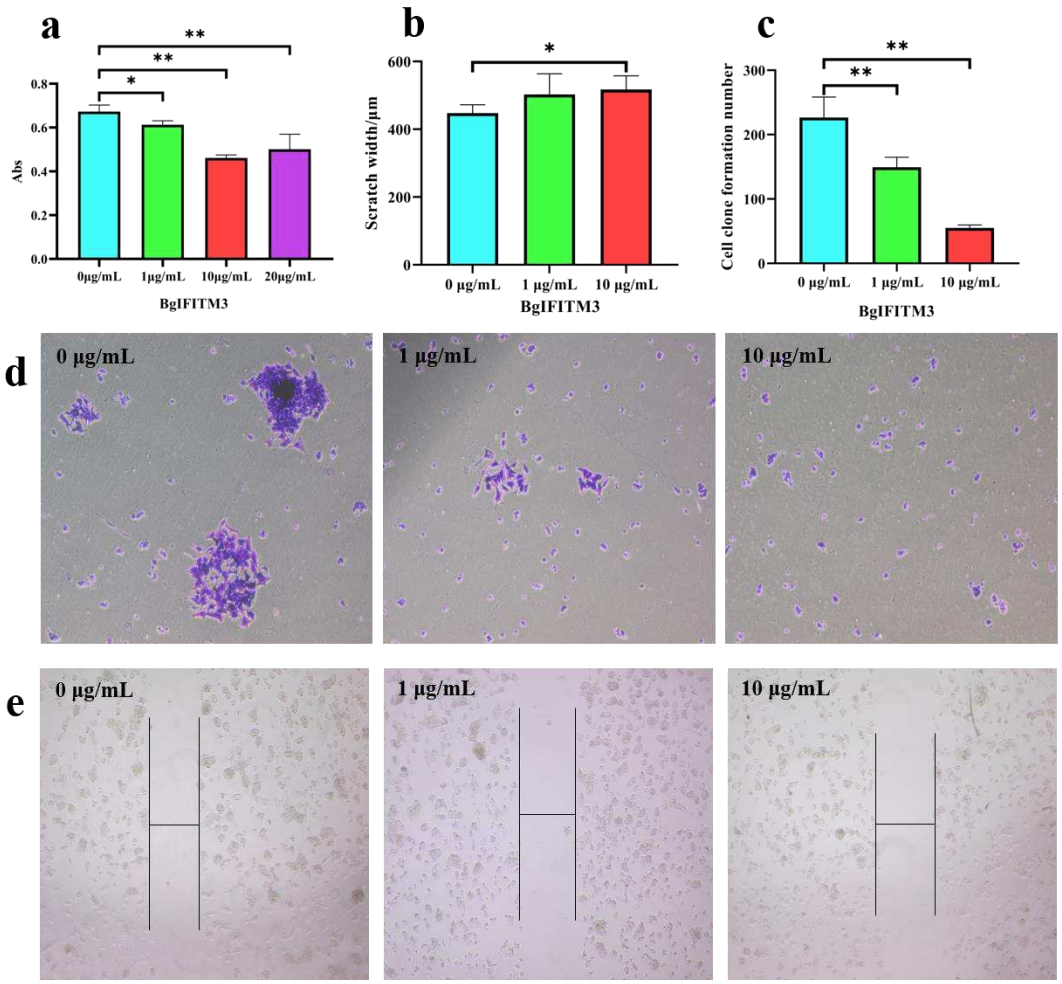

Fig. 6 The proliferation and migration of HepG2 cells. **a** HepG2 Cells Activity. **b** The scratch width of HepG2 cells. **c** The Number of Clones Formed in HepG2 Cells. **d** HepG2 cell clone formation. **e** HepG2 cell migration. Values are expressed as mean ± SD of n = 3. * P <0.05; ** P <0.01

The ultrastructure of HepG2 cells

The mitochondria of HepG2 cells were concentrated, Cristae widened and the double film density of mitochondria was increased after treating with 10 μg/mL BgIFITM3 protein. The above results indicated that the addition of BgIFITM3 protein decrease HepG2 cell activity may be caused by the ferroptosis mechanism (Fig. 7).

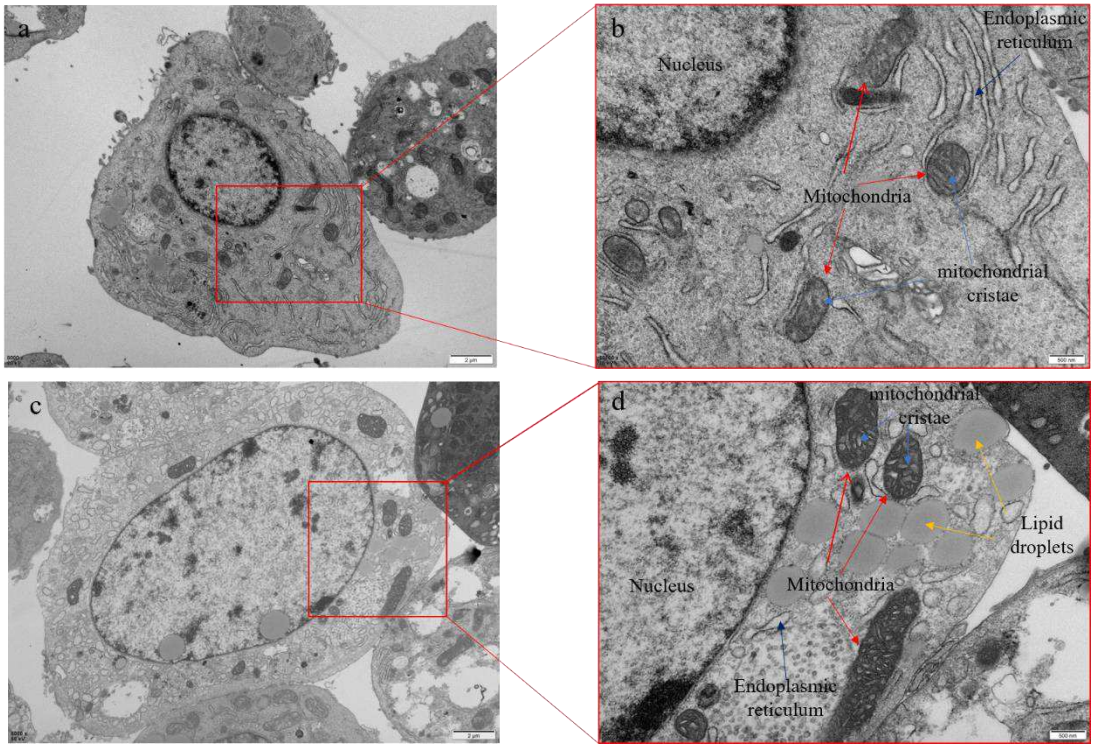

Fig. 7 Observation of HepG2 cells morphology by transmission electron microscope **a** Observation of normal HepG2 cells (8000×). **b** Observation of normal HepG2 cells (25000×). **c** Observation of HepG2 cells treated with BgIFITM3 protein (8000×). **d** Observation of HepG2 cells treated with BgIFITM3 protein (25000×)

Ferroptosis-related genes and migration-related in HepG2 cells

The expression of ferroptosis-related genes (*FTH-1*, *VDAC-2*, *VDAC-3*, *GPX-4* and *p53*) in HepG2 cells were detected by qRT-PCR. The results showed that the expression level of the *FTH-1* gene showed an upward trend with the increased of BgIFITM3 protein concentration (Fig. 8a). The expression levels of *VDAC-2*, *VDAC-3* and *p53* genes were significantly higher after treating with 10 μg/mL BgIFITM3 protein (P <0.01) (Fig. 8b-d). The expression level of *GPX-4* gene was significant lower after treating with BgIFITM3 protein (1 and 10 μg/mL) (P <0.05) (Fig. 8e). The expression of *MMP*2 and *MMP*9 mRNA level was extremely significant lower after treating with 10 μg/mL BgIFITM3 protein (P <0.01) (Fig. 8f-g).

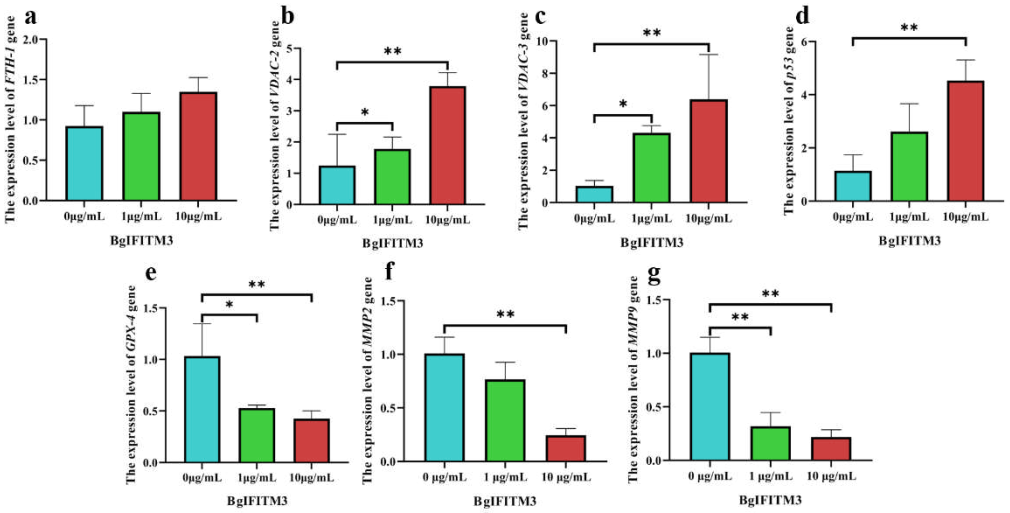

Fig. 8 The expression of related genes in HepG2 cells. **a** Expression of *FTH-1*. **b** Expression of *VDAC-2*. **c** Expression of *VDAC-3*. **d** Expression of *P53*. **e** Expression of *GPX-4*. **f** Expression of *MMP2*. **g** Expression of *MMP9*. Values are expressed as mean ± SD of n = 3. * P <0.05; ** P <0.01

Discussion

So far, *IFITM3* gene has been cloned in humans, mice, pigs, cattle, monkeys and other mammals **[30-34]**. The cattle and chicken IFITM3 protein contained a highly conserved structural-functional domain CD225 **[33, 35]**. In this study, the BgIFITM3 protein also contained the domain CD225. These reports showed that the *IFITM3* gene was highly conserved in different species. The above results indicated that the structure and conserved regions of IFITM3 may play a very important role in its function.

At present, there were a few reports about the transcription level of *IFITM*3 gene in various animal. IFITM3 was induced by interferon (IFN), which participated in the signal transduction pathway under hypoxia stress conditions and acted on a variety of immune cells to regulate the balance of the body **[36]**. Zebrafish *IFITM3* gene had the higher transcription level in the ovary, and lower in the liver, kidney, brain, muscle and testis **[37]**. Swine *IFITM3* gene had the highest transcription level in the spleen and lung, followed by higher in the kidney, and lower in the heart and liver **[38]**. Goose *IFITM3* gene had the highest transcription level in the lungs, followed by higher in the spleen and kidney, and lower in the heart and liver **[39]**. Rat *IFITM3* gene had the highest transcription level in the liver, followed by higher in the spleen and heart, and lower in the lung and kidney **[40]**. In this study, *BgIFITM3* gene was also the highest expressed in liver tissue. The transcription level of the *IFITM3* gene in each tissue has undergone significant changes with

the increase of age except the heart. Therefore, it was speculated that the differential expression of the *BgIFITM3* gene in various tissues might be participates in regulating the body's immune balance in a hypoxic environment. The reasons for these differences of above reports may be due to the species differences and living environment.

With the deepening of research on antiviral natural immunity, it has been found that interferon-induced transmembrane proteins can inhibit a variety of viral infections **[1]**. IFITM3 has been shown to restrict replication of around seventeen, mostly enveloped, RNA viruses including influenza A virus (IAV), HIV-1, Ebola, SARS coronavirus, and Dengue virus **[41]**. The research of human IFITM3 has made great progress, and it had inhibitory effects on a variety of viruses, but mainly using gene over expression or silencing **[42-45]**. The down-regulation of *IFITM3* significantly reduced c-myc expression and inhibited the proliferation of liver cancer in vitro and in vivo **[46]**. IFITM3 played a key role in the regulation of malignant tumor cell proliferation, invasion, and bone migration by TGF-β-Smads Signaling Pathway **[47]**. IFITM3 promotes hepatocellular carcinoma invasion and metastasis by regulating MMP9 through p38/MAPK signaling **[48]**. IFITM3 may a crucial mediator in TGF-β-induced glioma cells invasion and promote TGF-β-mediated glioma cells invasion through STAT3 activation **[49]**. IFITM3 knockdown led to reduced expressions of CCND1 and CDK4 and reduced RB phosphorylation, leading to inhibition of OSCC cell growth **[50]**.

IFITM3 can anti-proliferation, anti-virus and anti-tumor. Overexpression of the human *IFITM1* gene can significantly inhibit the growth of normal hepatocyte **[51]**. Pig HDCA suppressed intestinal epithelial cell proliferation through PI3K/Akt signaling pathway **[52]**. LncRNA FER1L4 suppressed cell proliferation and metastasis by inhibiting the PI3K/Akt signaling pathway in lung cancer **[53]**. Our study was the same as the above reports. Moreover, the BgIFITM3 protein can cause the ferroptosis of HepG2 cells. Ferroptosis is a newly discovered form of regulated cell death. The knockout of *GPX-4* causes cell death in a pathologically relevant form of ferroptosis in mice **[54]**. The *p53* expression was increased in PC12 cells will lead to ferroptosis **[55]**. The *FANCD2* was knockout will be decreased *FTH-1* and *GPX-4* expression to induced ferroptosis **[56]**. Erastin can regulate the increasing of *VDAC2/3* expression and inducing ferroptosis **[57]**. The results of this study are basically consistent with the above results.

Conclusion

In summary, we found that the BgIFITM3 protein mainly expressed in the yak liver. It could

inhibit the proliferation of hepatocyte by down-regulating the PI3K/Akt pathway, and it also could inhibit the activity of HepG2 cells by regulating ferroptosis-related genes.

Supplementary Information

Abbreviations

IFITM3: Interferon Induced Transmembrane Protein 3; ERBB2: Erb-B2 Receptor Tyrosine Kinase 2; IRS-1: Insulin Receptor Substrate 1; PI3KR-1: Phosphoinositide-3-Kinase Regulatory Subunit 1; AKT-1: AKT serine/threonine kinase 1; RAF-1: Raf-1 Proto-Oncogene, Serine/Threonine Kinase; MAPK-3: Mitogen Activated Protein Kinase 3; MMP-2: Matrix Metallopeptidase 2; MMP-9: Matrix Metallopeptidase 9; FTH-1: Ferritin Heavy Chain 1; VDAC-2: Voltage-Dependent Anion Channel 2; VDAC-3: Voltage-Dependent Anion Channel 3; GPX-4: Glutathione Peroxidase 4; GAPDH: Glyceraldehyde-3-Phosphate Dehydrogenase; qRT-PCR: Quantitative Real-time PCR.

Acknowledgements

The authors thanks Chengdu Medical College for providing HepG2 cells.

Authors' contributions

LW designed the study and revised manuscript. YZ and LZ carried out the induction and purification of the BgIFITM3 protein; JL and FF helped to cultivate the yak hepatocyte and HepG2 cells; HPW performed this study, analyzed the data and wrote the manuscript. All authors read and approved the final manuscript.

Funding

This work was financially supported by the innovative Postgraduate Project of Southwest University for Nationalities (CX2020SZ30) and Selected Funding Project for Science and Technology Activities of Overseas Students in Sichuan Province (2019).

Availability of data and materials

The data analyzed during the current study are available from the corresponding author on reasonable request.

Ethics approval and consent to participate

All animal experiments were performed according to the protocols approved by the Southwest Minzu University Institutional Animal Care and Use Committee. All animal procedures followed the regulations and guidelines established by this committee and minimized the suffering of animals.

Consent for publication

Not applicable.

Competing interests

The authors declare that they do not have any conflict of interest.

Author details

[1]Key Laboratory of Qinghai-Tibetan Plateau Animal Genetic Resource Reservation and Exploitation of Ministry of Education, Chengdu 610041, Sichuan, China. [2]Key Laboratory of Animal Science of State Ethnic Affairs Commission, Southwest Minzu University, Chengdu 610041, Sichuan, China.

References

1. Brass AL, Huang IC, Benita Y, John SP, Krishnan MN, Feeley EM, et al. The IFITM Proteins Mediate Cellular Resistance to Influenza A H1N1 Virus, West Nile Virus, and Dengue Virus. Cell. 2009; 139: 1243-1254.
2. Gobillot TA, Humes D, Sharma A, Kikawa C, Overbaugh J. The Robust Restriction of Zika Virus by Type-I Interferon in A549 Cells Varies by Viral Lineage and Is Not Determined by IFITM3. Viruses. 2020; 12: 503.
3. Diamond MS, Farzan M. The broad-spectrum antiviral functions of IFIT and IFITM proteins. Nat Rev Immunol. 2013; 13: 46–57.
4. Ahi YS, Yimer D, Shi GL, Majdoul S, Rahman K, Rein A, et al. IFITM3 Reduces Retroviral Envelope Abundance and Function and Is Counteracted by glycoGag. mBio. 2020; 11: 1-15.
5. Zou X, Yuan M, Zhang TY, Zheng N, Wu ZW. EVs Containing Host Restriction Factor IFITM3 Inhibited ZIKV Infection of Fetuses in Pregnant Mice through Trans-placenta Delivery. Mol Ther. 2020; 29: 1-15.
6. kenney A D, Mcmichael M, Imas A, Chesarino NM, Zhang LZ, Dorn LE, Wu Q, Alfaour O, Amari F, Chen M, Zani A, Chemudupati M, Accornero F, Coppola V, Rajaram MVS, Yount JS. IFITM3 protects the heart during influenza virus infection. PNAS. 2019; 116: 201900784.
7. Lei N, Li Y, Sun Q, Lu J, Zhou J, Li Z, et al. IFITM3 affects the level of antibody response after influenza vaccination. Emerg Microbes Infec. 2020; 9: 976-987.
8. Zhang AK, Duan H, Zhao HJ, Liao HC, Du YK, Li LL, et al. Interferon-induced transmembrane protein 3 is a virus-associated protein which suppresses porcine reproductive

and respiratory syndrome virus replication by blocking viral membrane fusion. J Virol. 2020; 94: e01350-20.

9. Sun X, Zeng H, Kumar A, Belser JA, Maines TR, Tumpey TM. Constitutively expressed IFITM3 protein in human endothelial cells poses an early infection block to human influenza viruses. J Virol. 2016; 90: 11157-11167.
10. Chesarino NM, Compton AA, McMichael TM, Kenney AD, Zhang L, Soewarna V, et al. IFITM3 requires an amphipathic helix for antiviral activity. EMBO Rep. 2017; 18: 1740-1751.
11. Bailey CC, Zhong G, Huang IC, Farzan M. IFITM-Family Proteins: The Cell's First Line of Antiviral Defense. Annu Rev Virol. 2014; 1: 261-283.
12. Rahman K, Coomer CA, Majdoul S, Ding SY, Padilla-Parra S, Compton AA. Homology-guided identification of a conserved motif linking the antiviral functions of IFITM3 to its oligomeric state. eLife. 2020; 9: e58537.
13. Wee YS, Roundy KM, Weis JJ, Weis JH. Interferon-inducible transmembrane proteins of the innate immune response act as membrane organizers by influencing clathrin and v-ATPase localization and function. Innate Immun. 2012; 18: 834-845.
14. Wu XJ, Spence JS, Das T, Yuan XQ, Chen CJ, Zhang YQ, et al. Site-Specific Photo-Crosslinking Proteomics Reveal Regulation of IFITM3 Trafficking and Turnover by VCP/p97 ATPase. Cell Chem Biol. 2020; 27: 571-585.
15. Du SW, Jiang YY, Xu W, Bai JY, Tian MY, Wang MP, et al. Construction, expression and antiviral activity analysis of recombinant adenovirus expressing human IFITM3 in vitro. Int J Biol Macromol. 2019; 131: 925-932.
16. Hur JY, Frost GR, Wu X, Crump C, Pan SJ, Wong E, et al. The innate immunity protein IFITM3 modulates γ-secretase in Alzheimer's disease. Nature. 2020; 586: 735-740.
17. Xu J, Qian P, Wu Q, Liu S, Fan W, Zhang K, et al. Swine interferon-induced transmembrane protein, sIFITM3, inhibits foot-and-mouth disease virus infection in vitro and in vivo. Antiviral Res. 2014; 109: 22-9.
18. Blyth GA, Chan WF, Webster RG, Magor KE. Duck Interferon-Inducible Transmembrane Protein 3 Mediates Restriction of Influenza Viruses. J Virol. 2015; 90: 103-16.
19. Smith J, Smith N, Yu L, Paton IR, Gutowska MW, Forrest HL, et al. A comparative analysis of host responses to avian influenza infection in ducks and chickens highlights a role for the

interferon-induced transmembrane proteins in viral resistance. BMC Genomics. 2015; 16: 574.

20. Li D, Peng Z, Tang H, Wei P, Kong X, Yan D, et al. KLF4-mediated negative regulation of IFITM3 expression plays a critical role in colon cancer pathogenesis. Clin Cancer Res. 2011; 17: 3558-3568.
21. Zhao B, Wang H, Zong G, Li P. The role of IFITM3 in the growth and migration of human glioma cells. BMC Neurol. 2013; 13: 210.
22. Seyfried NT, Huysentruyt LC, Atwood JA, Xia Q, Seyfried TN, Orlando R. Up-regulation of NG2 proteoglycan and interferon-induced transmembrane proteins 1 and 3 in mouse astrocytoma: a membrane proteomics approach. Cancer Lett. 2008; 263: 243-252.
23. Min J, Hu J, Luo C, Zhu J, Zhao J, Zhu Z, et al. IFITM3 upregulates c-myc expression to promote hepatocellular carcinoma proliferation via the ERK1/2 signalling pathway. Biosci Trends. 2020; 13: 523-529.
24. Carter BD, Kaltschmidt C, Kaltschmidt B, Offenhäuser N, Böhm-Matthaei R, Baeuerle PA, et al. Selective activation of NF-kappa B by nerve growth factor through the neurotrophin receptor p75. Science. 1996; 272: 542-5.
25. Wu TY, Ding SQ, Zhang SL, Duan JQ, Li BY, Zhan ZY, et al. Altitude illness in Qinghai–Tibet railroad passengers. High Alt Med Biol. 2010; 11: 189-98.
26. Timpl P, Spanagel R, Sillaber I, Kresse A, Reul JM, Stalla GK, et al. Impaired stress response and reduced anxiety in mice lacking a functional corticotropin-releasing hormone receptor 1. Nat Genet. 1998; 19: 162-6.
27. Jia W, Zhang R, Shi L, Zhang F, Chang J, Chu XG. Accurate determination of volatile-flavor components in bos grunniens milk by high-throughput dynamic headspace gas chromatographic-mass spectrometry. J Chromatogr A. 2019; 1603: 67-82.
28. Qiu Q, Zhang GJ, Ma T, Qian WB, Wang JY, Ye ZQ, et al. The yak genome and adaptation to life at high altitude. Nat Genet. 2012; 44: 946-951.
29. Goshu HA, Chu M, Xiaoyun W, Pengjia B, Zhi DX, Yan P. Genomic copy number variation of the CHKB gene alters gene expression and affects growth traits of Chinese domestic yak (Bos grunniens) breeds. Mol Genet Genomics. 2019; 294: 549-561.
30. Lewin AR, Reid LE, McMahon M, Stark GR, Kerr IM. Molecular analysis of a human interferon-inducible gene family. Eur J Biochem. 1991; 199: 417-23.

31. Saitou M, Barton SC, Surani MA. A molecular programme for the specification of germ cell fate in mice. Nature. 2002; 418:293-300.
32. Uenishi H, Eguchi T, Suzuki K, Sawazaki T, Toki D, Shinkai H, et al. PEDE (Pig EST Data Explorer): construction of a database for ESTs derived from porcine full-length cDNA libraries. Nucleic Acids Res. 2004; 32: D484-8.
33. Zimin AV, Delcher AL, Florea L, Kelley DR, Schatz MC, Puiu D, et al. A whole-genome assembly of the domestic cow, Bos taurus. Genome Biol. 2009; 10: R42.
34. Winkler M, Gärtner S, Wrensch F, Krawczak M, Sauermann U, Pöhlmann S. Rhesus macaque IFITM3 gene polymorphisms and SIV infection. PLoS One. 2017; 12: e0172847.
35. HKim YC, Jeong MJ, Jeong BH. Genetic characteristics and polymorphisms in the chicken interferon-induced transmembrane protein (IFITM3) gene. Vet Res Commun. 2019; 43: 203-214.
36. Hu Y, Li M, Lu B, Wang X, Chen C, Zhang M. Corticotropin-releasing factor augments LPS-induced immune/inflammatory responses in JAWSII cells. Immunol Res. 2016; 64: 540-7.
37. Xue WW, Wang HN, Wang ZM, Qiu MX, Che J, Deng FJ, et al. Cloning and characterization of ifitm1 and ifitm3 expression during early zebrafish development. Zygote. 2016; 24: 149-58.
38. Li HP, Chen PG, Liu FT, Zhu HS, Jiao XQ, Zhong K, et al. Characterization and anti-inflammation role of swine IFITM3 gene. Oncotarget. 2017; 8: 73579-73589.
39. Wang A, Sun L, Wang M, Jia R, Zhu D, Liu M, et al. Identification of IFITM1 and IFITM3 in Goose: Gene Structure, Expression Patterns, and Immune Reponses against Tembusu Virus Infection. Biomed Res Int. 2017; 2017: 5149062.
40. Lu Y, Zuo Q, Zhang Y, Wang Y, Li T, Han J. The expression profile of IFITM family gene in rats. Intractable Rare Dis Res. 2017; 6: 274-280.
41. Huang IC, Bailey CC, Weyer JL, Radoshitzky SR, Becker MM, Chiang JJ, et al. Distinct patterns of IFITM-mediated restriction of filoviruses, SARS coronavirus, and influenza A virus. PLoS Pathog. 2011; 7: e1001258.
42. Hu J, Wang S, Zhao Y, Guo Q, Zhang D, Chen J, et al. Mechanism and biological significance of the overexpression of IFITM3 in gastric cancer. Oncol Rep. 2014; 32: 2648-56.
43. Jia Y, Zhang M, Jiang W, Zhang Z, Huang S, Wang Z. Overexpression of IFITM3 predicts the high risk of lymphatic metastatic recurrence in pN0 esophageal squamous cell carcinoma after

Ivor-Lewis esophagectomy. PeerJ. 2015; 3: e1355.

44. Gan CP, Sam KK, Yee PS, Zainal NS, Lee BKB, Abdul Rahman ZA, et al. IFITM3 knockdown reduces the expression of CCND1 and CDK4 and suppresses the growth of oral squamous cell carcinoma cells. Cell Oncol (Dordr). 2019; 42: 477-490.
45. Zhao B, Wang H, Zong G, Li P. The role of IFITM3 in the growth and migration of human glioma cells. BMC Neurol. 2013 Dec 27; 13: 210.
46. Min J, Hu J, Luo C, Zhu J, Zhao J, Zhu Z, et al. IFITM3 upregulates c-myc expression to promote hepatocellular carcinoma proliferation via the ERK1/2 signalling pathway. Biosci Trends. 2020; 13: 523-529.
47. Liu X, Chen L, Fan Y, Hong Y, Yang X, Li Y, et al. IFITM3 promotes bone metastasis of prostate cancer cells by mediating activation of the TGF-β signaling pathway. Cell Death Dis. 2019; 10: 517.
48. Min J, Feng Q, Liao W, Liang Y, Gong C, Li E, et al. IFITM3 promotes hepatocellular carcinoma invasion and metastasis by regulating MMP9 through p38/MAPK signaling. FEBS Open Bio. 2018; 8: 1299-1311.
49. Wang H, Tang F, Bian E, Zhang Y, Ji X, Yang Z, et al. IFITM3/STAT3 axis promotes glioma cells invasion and is modulated by TGF-β. Mol Biol Rep. 2020; 47: 433-441.
50. Gan CP, Sam KK, Yee PS, Zainal NS, Lee BKB, Abdul Rahman ZA, et al. IFITM3 knockdown reduces the expression of CCND1 and CDK4 and suppresses the growth of oral squamous cell carcinoma cells. Cell Oncol (Dordr). 2019; 42: 477-490.
51. Yang GH. Functional analysis of IFITM1 Gene in antiproliferative action of interferon-gamma. Chinese Academy of Sciences; 2006. (in Chinese)
52. Song M, Yang Q, Zhang F, Chen L, Su H, Yang X, et al. Hyodeoxycholic acid (HDCA) suppresses intestinal epithelial cell proliferation through FXR-PI3K/AKT pathway, accompanied by alteration of bile acids metabolism profiles induced by gut bacteria. FASEB J. 2020; 34: 7103-7117.
53. Gao X, Wang N, Wu S, Cui H, An X, Yang Y. Long non-coding RNA FER1L4 inhibits cell proliferation and metastasis through regulation of the PI3K/AKT signaling pathway in lung cancer cells. Mol Med Rep. 2019; 20: 182-190.
54. Friedmann Angeli JP, Schneider M, Proneth B, Tyurina YY, Tyurin VA, Hammond VJ, et al.

Inactivation of the ferroptosis regulator Gpx4 triggers acute renal failure in mice. Nat Cell Biol. 2014; 16: 1180-91.

55. Lu J, Xu F, Lu H. LncRNA PVT1 regulates ferroptosis through miR-214-mediated TFR1 and p53. Life Sci. 2020; 260: 118305.

56. Song X, Xie Y, Kang R, Hou W, Sun X, Epperly MW, et al. FANCD2 protects against bone marrow injury from ferroptosis. Biochem Biophys Res Commun. 2016; 480: 443-449.

57. Yagoda N, von Rechenberg M, Zaganjor E, Bauer AJ, Yang WS, Fridman DJ, et al. RAS-RAF-MEK-dependent oxidative cell death involving voltage-dependent anion channels. Nature. 2007; 447: 864-8.

Figures

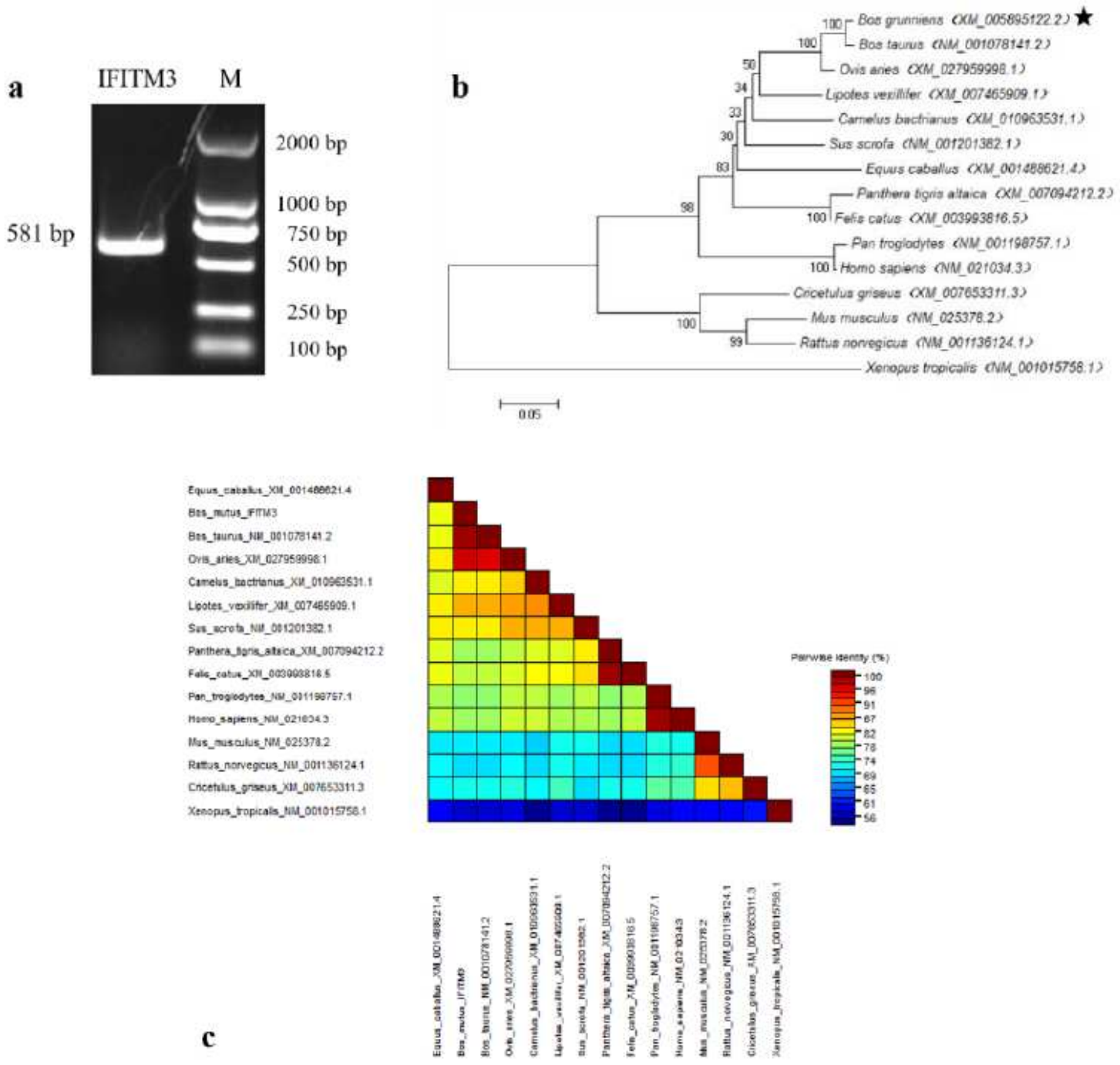

Figure 1

Analysis of BgIFITM3 Gene. a Result for PCR amplification of BgIFITM3. Note: M. DL2000 DNA Marker; IFITM3. BgIFITM3 gene. b Phylogenetic tree based on IFITM3 gene. c The nucleotide sequences of IFITM3 from various species were compared by pairwise alignment

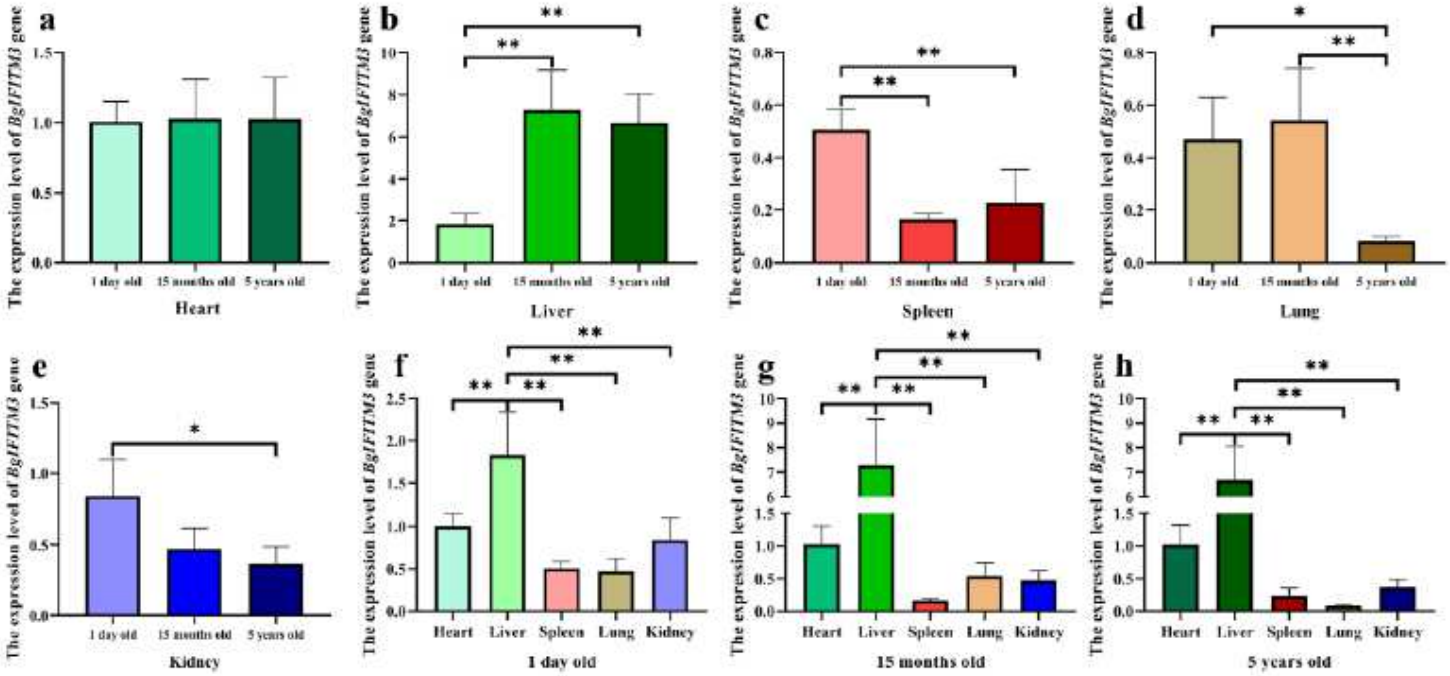

Figure 2

The expression levels of BgIFITM3 in different tissues of the yak. a The expression level of BgIFITM3 gene in heart. b The expression level of BgIFITM3 gene in liver. c The expression level of BgIFITM3 gene in spleen. d The expression level of BgIFITM3 gene in lung. e The expression level of BgIFITM3 gene in kidney. f The expression level of BgIFITM3 gene in 1 day old. g The expression level of BgIFITM3 gene in 15 months old. h The expression level of BgIFITM3 gene in 5 years old. Values are expressed as mean ± SD of n = 3. * P <0.05, ** P <0.01

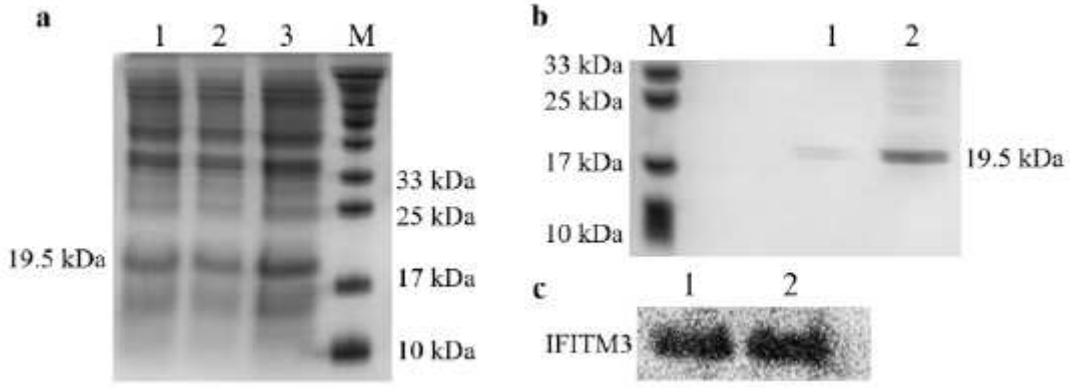

Figure 3

Prokaryotic expression and identification of recombinant protein IFITM3. a Graph of BgIFITM3 protein induction. Note: M: The low molecular weight standard markers; 1-3: The precipitation pET28a-BgIFITM3/DE3 induced for 12 h. b Graph of BgIFITM3 protein purification. Note: M: The low molecular weight standard markers; 1-2: The purified recombinant protein pET28a-BgIFITM3. c Graph of BgIFITM3

protein identification. Note: M: The low molecular weight standard markers; 1-2: The recombinant protein BgIFITM3

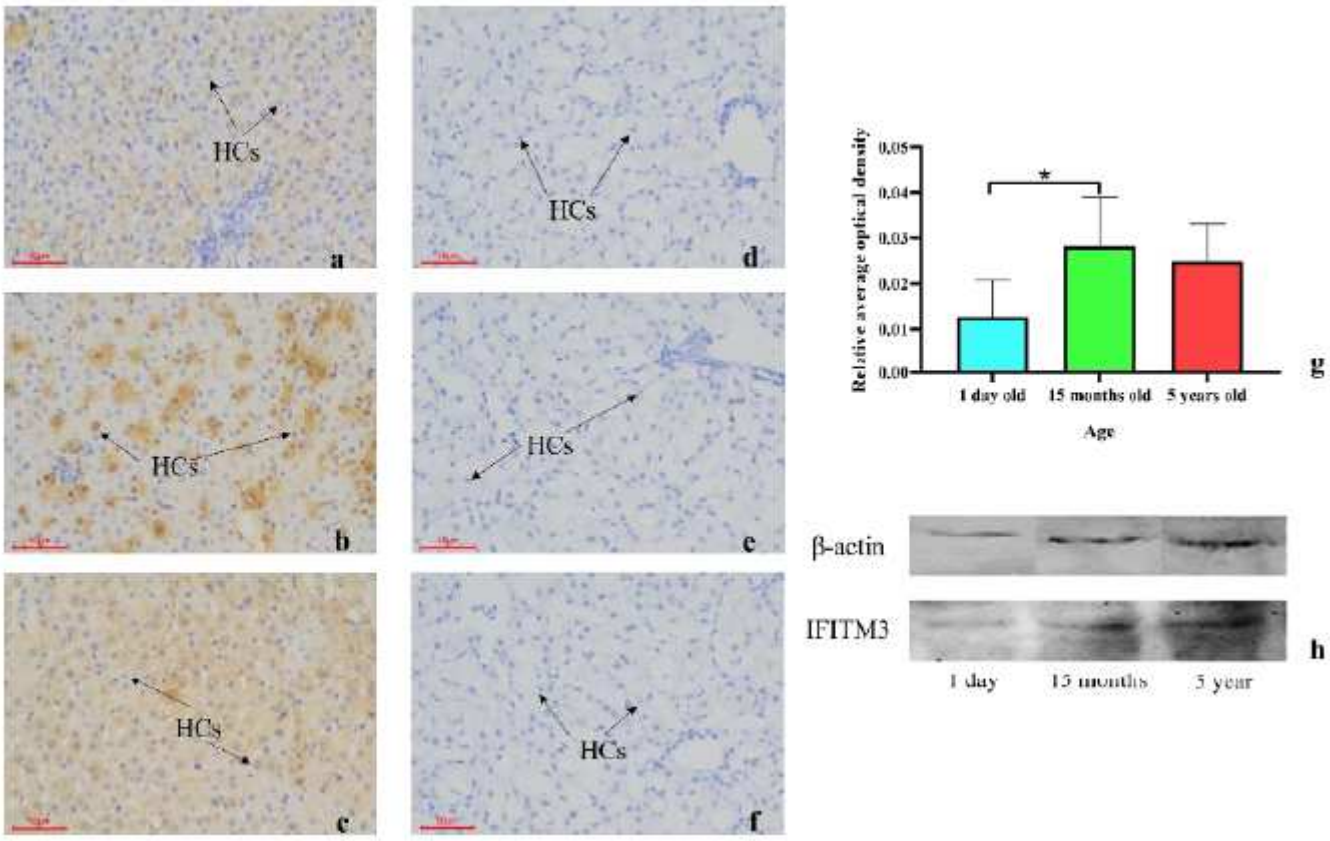

Figure 4

Detection of IFITM3 expression distribution in yak liver tissues at different growth stages. a-f Cell localization of BgIFITM3 protein. a 1-day-old yak liver (200×). b 15-month-old yak liver (200×). c 5-year-old yak liver (200×). d Group a negative control. e Group b negative control. f Group c negative control. g Relative average optical density. h The expression level of IFITM3 protein in yak at different ages. HCs: Hepatocyte. Values are expressed as mean ± SD of n = 3. * P <0.05

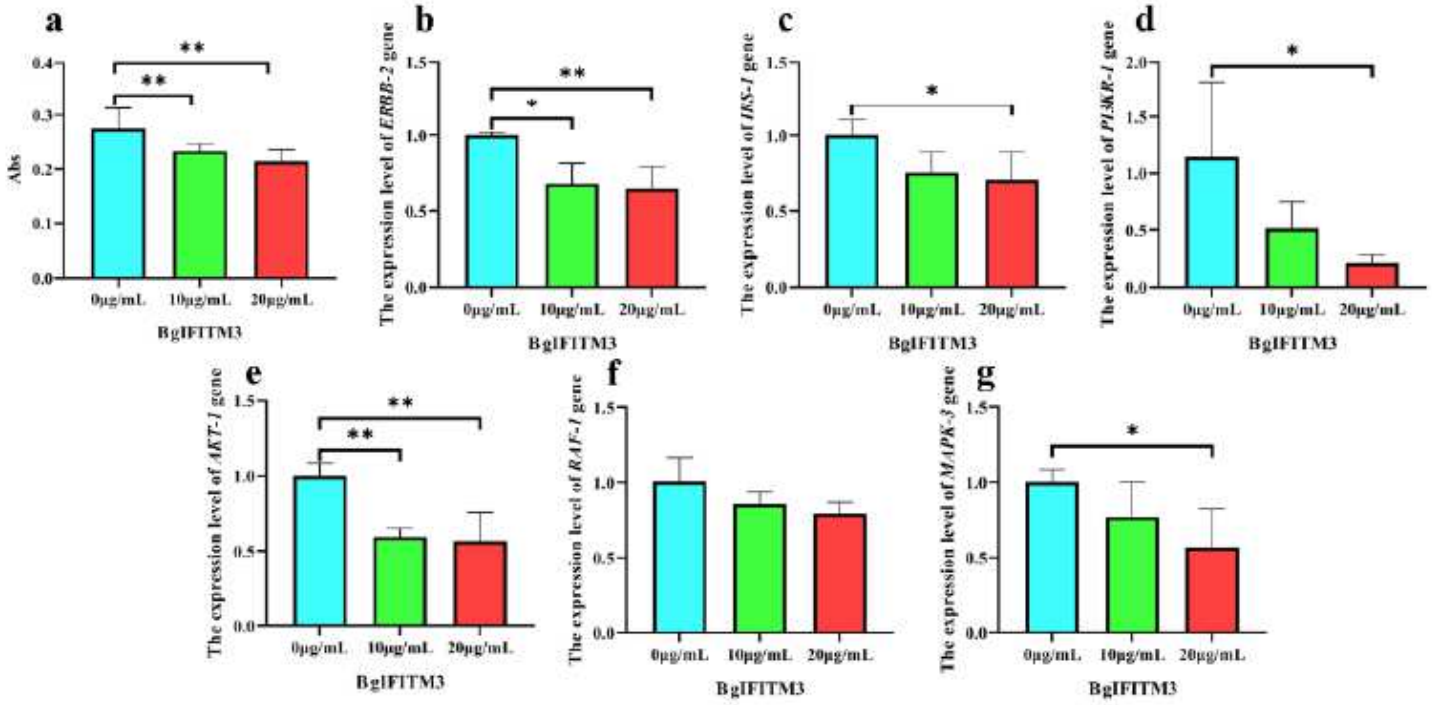

Figure 5

Effects of different concentrations of BgIFITM3 protein on yak hepatocyte a The yak hepatocyte activity. b Expression of ERBB-2. c Expression of IRS-1. d Expression of PI3KR-1. e Expression of AKT-1. f Expression of RAF-1. g Expression of MAPK-3. Values are expressed as mean ± SD of n = 3. * P <0.05, ** P <0.01

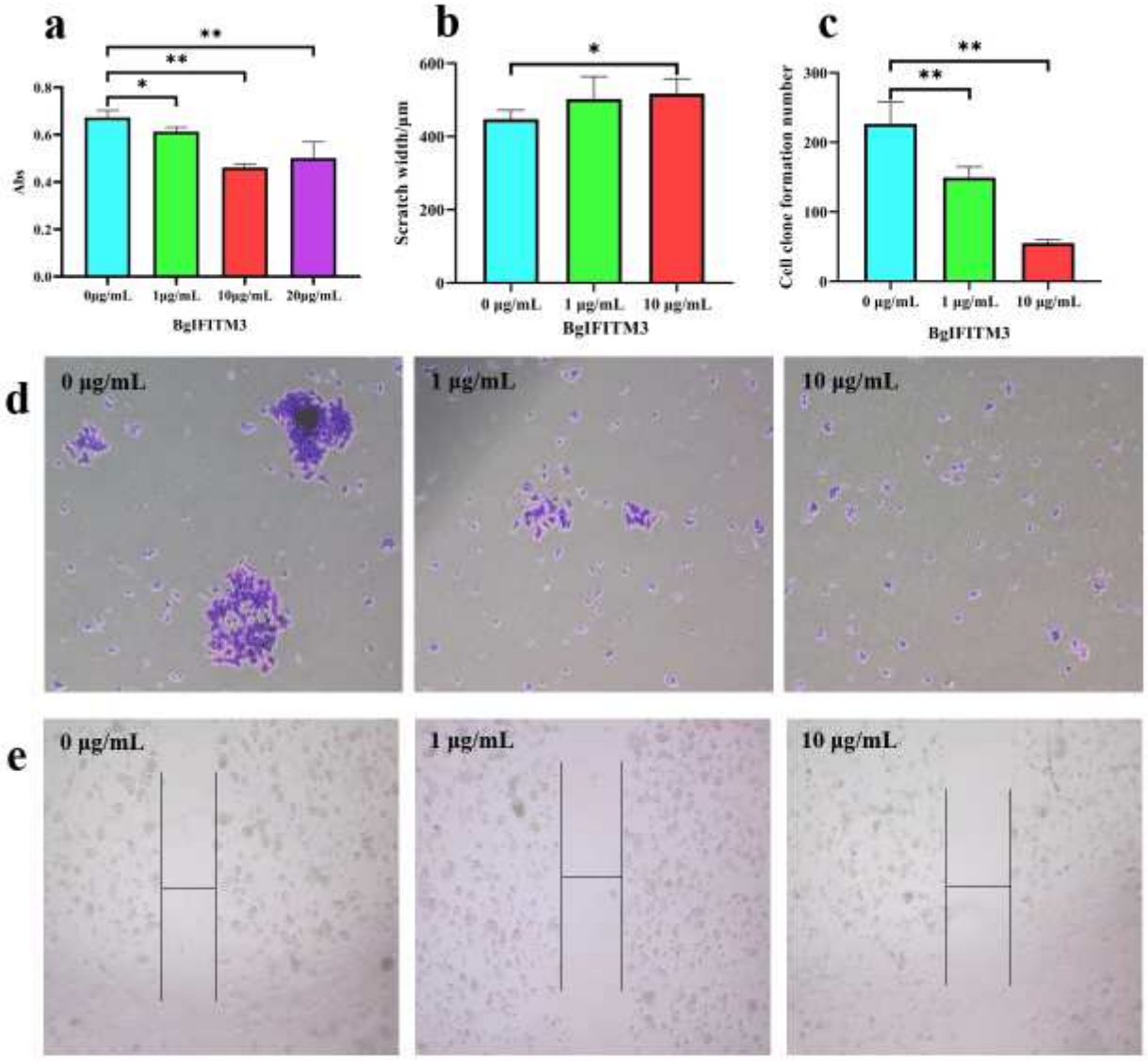

Figure 6

The proliferation and migration of HepG2 cells. a HepG2 Cells Activity. b The scratch width of HepG2 cells. c The Number of Clones Formed in HepG2 Cells. d HepG2 cell clone formation. e HepG2 cell migration. Values are expressed as mean ± SD of n = 3. * P <0.05; ** P <0.01

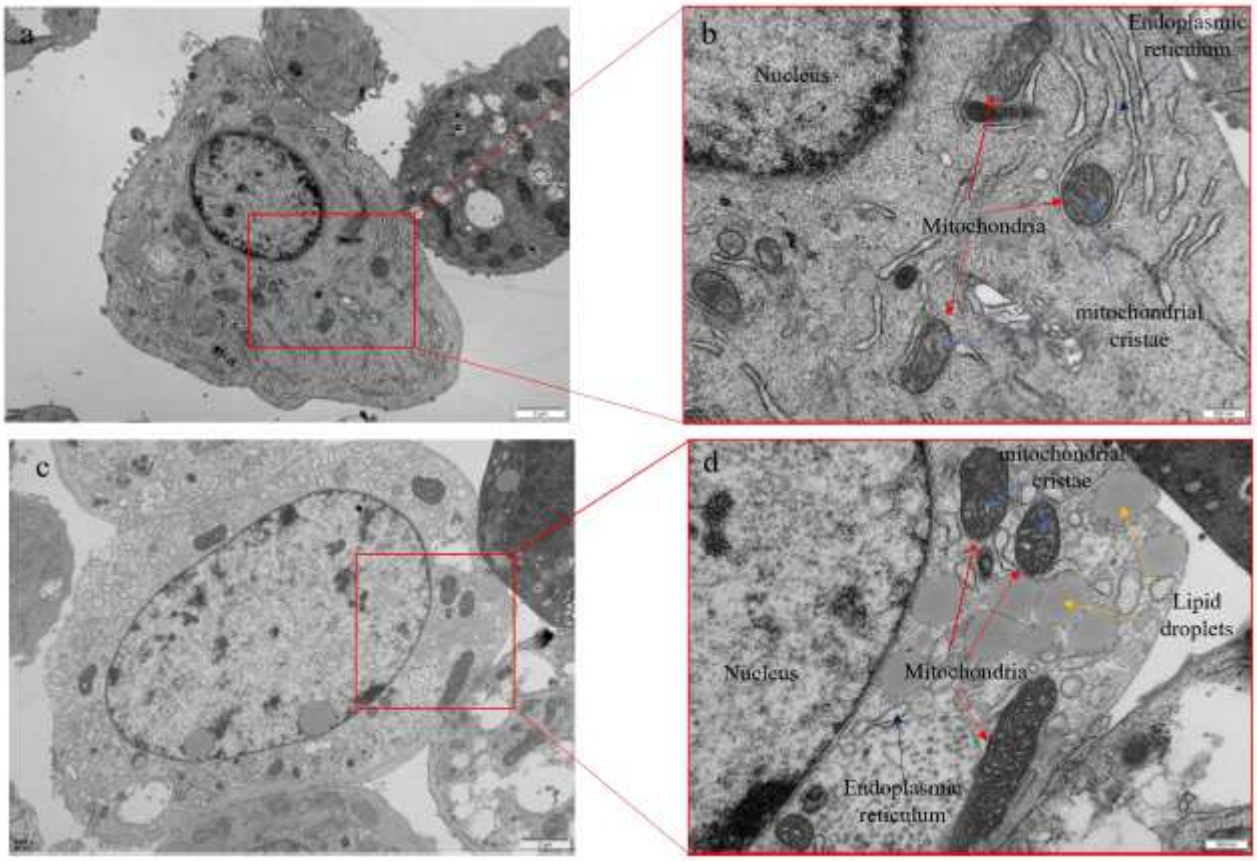

Figure 7

Observation of HepG2 cells morphology by transmission electron microscope a Observation of normal HepG2 cells (8000×). b Observation of normal HepG2 cells (25000×). c Observation of HepG2 cells treated with BgIFITM3 protein (8000×). d Observation of HepG2 cells treated with BgIFITM3 protein (25000×)

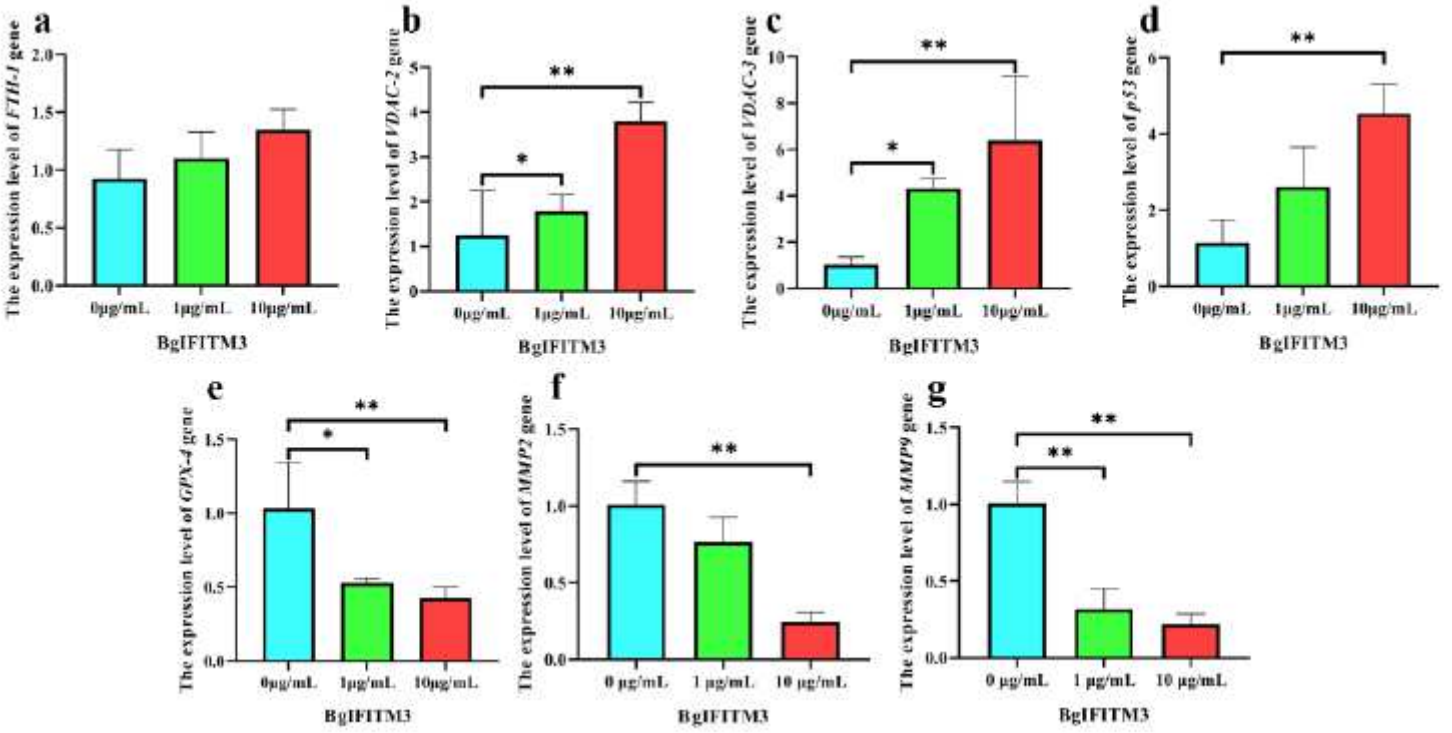

Figure 8

The expression of related genes in HepG2 cells. a Expression of FTH-1. b Expression of VDAC-2. c Expression of VDAC-3. d Expression of P53. e Expression of GPX-4. f Expression of MMP2. g Expression of MMP9. Values are expressed as mean ± SD of n = 3. * P <0.05; ** P <0.01